Biomechanical effects of different lumbar fusion cage designs

Rafael João Gonçalves Durão Guerreiro
rafael.guerreiro@tecnico.ulisboa.pt

Instituto Superior Técnico, Lisboa, Portugal

October 2018

Abstract

The lumbar column is a common place for diseases like low back pain to occur due to its role in weight support. This condition affects a large portion of the population and comes associated with a large economic burden to the patients and to the countries' economy. Lumbar interbody fusion is a type of surgery used in the treatment of these conditions and it involves the replacement of the intervertebral disc by an implant. The motivation for this study comes directly from the fact that, sometimes, the placement of this intervertebral cages results in comorbidities to the patient that should be avoided. The present study had two main goals: i) development of a new modifiable Finite Element (FE) model of the human L4-L5 segment and ii) development of new designs of the Synfix-LR system that would require less space to be inserted and result in a lower risk for the surgeon, while having the same biomechanical performance as the existent design. This study raised attention for the fact that the development of fixation systems for lumbar spinal cages that require less complex surgical access is of major importance. The FE simulations have shown that new designs can be created without resulting in a significant change of the biomechanical parameters observed for the original design, which was proved to be essential for the biomechanical performance of both spinal adjacent levels and implant. Further developments can bring light to the wide comparison of different fixation systems in various time points post implantation.

Keywords: Low Back Pain; Lumbar Interbody Fusion; Intervertebral Disc; Intervertebral Cages; Fixation System; Finite Elements

1. Introduction

Low Back Pain (LBP) is a very common condition that affects the inferior portion of the spine. Due to the major role that the spine plays in weight support and movement in the daily activities, this condition is a primary source of pain. Recent studies show that around 80% of the world population will suffer from LBP at some point in life. Being considered the major cause of activity limitation and work absence around the world, it comes associated with high costs to the patients and to the countries' economy (due to work absence and reduced productivity) [1, 2, 3].

Despite having multiple possible causes, recent studies have shown that LBP might occur as a symptom of a Degenerative Disc Disease (DDD). A common cause of this condition is an age-related wear and tear of the disc. Therefore, the Intervertebral Disc (IVD) is a common treatment target in order to prevent, reduce, or even eliminate LBP. The wide range of treatments include medication, massage therapy, physical therapy, and, in cases of severe and debilitating DDD, surgical treatment [4].

For the cases in which LBP persists for more than 6-12 weeks of non-surgical treatments (medication, massage therapy and others), the following are three of the main types of surgery that are usually performed (individually or combined): Lumbar Decompression, Lumbar Spinal Fusion, and Lumbar Total Disc Arthroplasty. Independently of what the chosen method is, the main goal is always to maintain the original function of the segments, and advantages and disadvantages exist for each method [5].

Even after a Lumbar Spinal Fusion is performed, lesions can occur in the discs adjacent to the fused region. In a study conducted by Ishihara, symptomatic adjacent segment disease was diagnosed to 9 of the 112 patients being followed up (approximately 17%). Additionally, 7 out of the 9 patients needed a second surgery to correct this condition [6]. Since most of the modern cages are fixed to the vertebral bodies by a set of screws, it is of major importance to study new designs and configurations that can help reduce the number of cases of adjacent segment disease. When developing a new cage or a new screw configuration, its ease of placement by the surgeon must be taken into consideration, since an incorrect positioning of the cage can lead to lower levels of interbody fusion and even to the migration of the cage [7]. Therefore, two main objectives were set for this study:

1. The first goal was the development and validation of a new FE model of a L4-L5 segment. The main goal was to keep the geometry of the model as simple as possible while making it efficient and robust;

2. The second main objective was to propose new cage designs that could be more easily implanted without compromising its performance. The biomechanical effects of several cage designs were studied using the newly developed model of the L4-L5 segment.

2. Background

Since it first appeared in the 20th century as a treatment to several disorders affecting the lumbar spine, the techniques used in the lumbar spinal fusion surgery have changed and several types of different procedures can be conducted. Nowadays, a surgery can be performed as an Anterior Lumbar interbody Fusion (ALIF), a Posterior lumbar Interbody Fusion (PLIF) or even by a Lateral Lumbar Interbody Fusion (LLIF). The type of approach used depends on the technical ability of the surgeon, on the patient's pathology, the size and orientation of the implant, amongst other factors [8]. Even though these approaches are different, the goal is always to be able to remove the IVD or a part of it, to prepare the bone graft and to correctly insert the implant in order to restore the normal height of the disc and the correct alignment of the spine [9]. The ALIF approach, which was considered in this study, consists in a retroperitoneal approach that allows the surgeon to be exposed to the anterior spine. However, there is an increase of the risk of a vascular or ureteral injury. Besides the fact that it allows the direct exposure of the anterior portion of the spine, one of the biggest advantages of an ALIF approach is that the surgeon does not have to dissect any of the paraspinal muscles, reducing the postoperative pain [9].

The first techniques to perform intervertebral body fusion were introduced by Robinson and Smith in the 1950s. This procedure involved an initial distraction, anterior decompression of the segment and the insertion of a horseshoe graft that had been previously obtained from the patient's iliac crest. This graft provided the ideal conditions to the growth of new bone that would lead to the total stabilization of the affected segment. However, due to several problems associated with the autogenous graft harvesting (infection, nerve injury, and iliac crest fractures), other alternatives for the grafts' materials had to be found. Despite the efforts, autografts continued to present the best results in fusion. Consequently, the focus of the investigation changed to cage implants as alternatives to the bone grafts [10].

This new fusion technique using a cage implant was firstly proposed by Bagby in 1988 . This cage, named Bagby bone basket, consisted of a 30mm long cylinder fabricated in a fenestrated and hollow stainless steel that allows the bone to grow to its inside. The following figure shows this first cage design [11]:

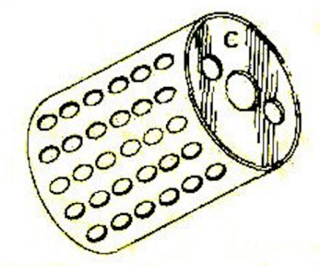

Figure 1: Illustration of a Bagby Bone Basket. Adapted from [11].

Nowadays, multiple designs, heights, widths, materials, and fixation methods are available for the cages. In relation to the materials available, three have been primarily used: Titanium and its alloys, Polyetheretherketone (PEEK) and ceramics [12]. The designs of the cages can also be divided in threaded, having a shape similar to a screw, and non-threaded (vertical rings and cages with a box shape), with each design having its own advantages and disadvantages [10].

3. Implementation

3.1. Intact Model

One of the main goals of this study was the development of a new FE model of the human L4-L5 segment. This model had to be robust and efficient while being easily computed. For this purpose, only the vertebral body was considered, while the ligaments, the muscles and all the structures that form the neural arch, were not included.

The model was built using SOLIDWORKS® (Student Edition, Academic Year 2016-2017).

The final model of the L4-L5 segment is shown in the Figure 2.

After its construction, the model was imported to the FE solver ABAQUS® (Dassault Systmes Simulia Corp., USA) in order to perform several FE analyses. The main goal of this first analyses was to choose the best set of properties for the model, specially for the IVD. Considering that one of the main objectives of this work was to propose a new model with a low level of complexity, a solution that could

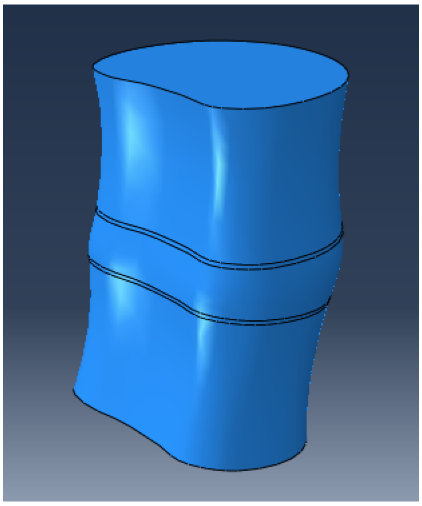

Figure 2: L4-L5 segment with two equal vertebrae and the IVD.

mimic the behavior of the fibers that are present in the IVD, mainly in the Annulus Fibrosus (AF), had to be found. Since these fibers increase the average stiffness of the structure where they are embedded, the adopted solution was to increase the Young Modulus of the AF and to define it as an anisotropic material, having higher stiffness according to the fibers directions. An *in vitro* study by Heuer et al. [13] was used to validate the model. The change in the lordosis angle and the Range of Motion (RoM) were analyzed but only the latter was used to compare with the numerical calculations of the present study.

It was found that the predictions observed for the initial set of properties were not in the range of values observed by Heuer et al. In order to achieve comparable results, a number of material properties sets were attributed to the AF (while the properties of the other structures were kept constant) and the predictions were again compared to the *in vitro* results. To do so, the parameters k_1, k_2 and $kappa$ were kept constant, while C_{10}, and consequently D_1, were changed. C_{10} was increased 50%, 75%, 100%, 150%, 175% and 200%, and the outcomes that came closer to the *in vitro* results were obtained for the 75% increase.

For the 75% increase, 17 outcomes out of the total 20 (5 for each physiological motion) were found to be in agreement with the results observed by Heuer et al. This agreement was verified every time a numerical outcome fell within the range min-max described in the *in vitro* study. The 3 cases in which the predictions were not in the range are: 1 Nm of flexion, 10 Nm of axial rotation, and 10 Nm of lateral bending.

After optimization and validation, the best set of material properties was found to be the one presented in Table 1. The material properties shown in this table were then used in the simulations that were performed with the final intact model. The predictions of these FE simulations are then compared with those of the instrumented models.

3.2. Convergence Study

After the optimization process of the material properties of the AF, a convergence study was conducted to ensure that the predictions of the FE analyses were not influenced by the size and type of elements that were being used. Therefore, the assembly was meshed with five different element sizes and the Von Mises stress was studied in two distinct points of the segment (center of the IVD and center of the upper vertebra). The analyses were carried out with ten nodes quadratic tetrahedral elements (C3D10). The element sizes considered in the convergence study were 4 mm (15603 elements and 22401 nodes), 3.5 mm (21939 elements and 31177 nodes), 3 mm (30851 elements and 43656 nodes), 2.5 mm (50533 elements and 70976 nodes) and 2 mm (87736 elements and 122526 nodes). After analyzing the evolution of the Von Mises stress with the number of nodes and, consequently, with the simulation cost, the chosen seed size was 2.5 mm.

3.3. Instrumented Models

As mentioned before, one of the main goals of this study was the development of a new stable fixation system for the stand-alone ALIF cage Synfix LR (Synthes, Oberdorf, Switzerland). This implant is composed of a PEEK spacer and a titanium plate with four divergent locking screws for fixation. It has a zero profile construct, meaning that the PEEK spacer and the anterior fixation system fit totally inside the intervertebral space, decreasing the risk of a possible damage to the surrounding tissues and vessels. Its four divergent screws ensure the stability of the cage and a load transfer near the cortex of the vertebrae. One of the most common difficulties associated with this device is the correct positioning of the four screws. Due to the angle at which the screws are positioned, it requires a significant amount of space to correctly insert them. While inserting the screws, the surgeon has to move the surrounding structures, including several main vessels, more extensively than what is necessary for "standard" ALIF procedures. Several studies can be found in the literature reporting cases of operative lesions, such as: laceration of different vessels, thrombophlebitis, thrombotic occlusions of the iliac veins and iliac arteries, among others. From these studies, it was estimated that 0%-15% of the ALIF procedures result in vascular complications [16, 17]. The new fixation systems would have to require less space to be inserted, while obtaining the same results as the original model. Seven new designs were

Table 1: Material properties after optimization and validation.

Material	Formulation	Parameters	Reference
Cortical Bone	Linear Elastic	E = 12000 MPa	[14]
		ν = 0.3	
Trabecular Bone	Linear Elastic	E = 200 MPa	
		ν =0.315	
Cartilaginous Endplates	Linear Elastic	E = 23.8 MPa	
		ν = 0.4	
Nucleus Pulposus	Hyperelastic Isotropic (Mooney-Rivlin)	C_{10} = 0.12	
		C_{01} = 0.03	
		D_1 = 0.6667	
Annulus Fibrosus	Hyperelastic Anisotropic (Holzapfel)	C_{10} = 0.315	Current work
		D_1 = 0.2540	
		k_1 = 12 MPa	[15]
		k_2 = 300	
		$kappa$ = 0.1	Current work

created by changing the number of screws and the angle in which they are inserted and its description is shown in Table 2. As can be seen from the original design shown in Figure 3, some simplifications had to be made on the models in order to simplify the numerical calculations and, therefore, decrease the simulation time. These simplifications include: absence of spikes on the upper and lower surfaces of the PEEK spacer and absence of the screws' threads.

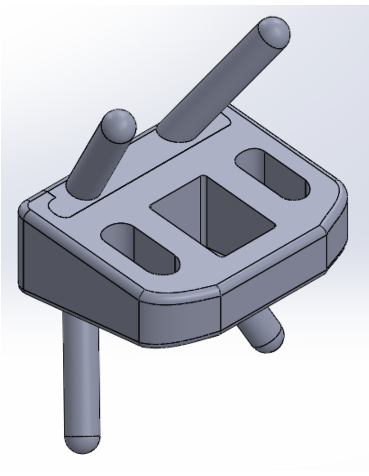

Figure 3: Isometric view of the original design of the Synfix-LR system.

To test the effects of the different Synfix-LR models, all the models were subjected to the same conditions. Firstly, the IVD (NP, AF and cartilaginous endplates) was removed in SOLIDWORKS® for all the models and only the vertebral bodies were kept in the instrumented models. Then, the implants were placed in the intervertebral space as described in the Technique Guide of the Synfix-LR system [18]. Again using SOLIDWORKS®, the vertebral bodies were cut by the implants to open space for the screws. Then, the models were imported to the FE solver ABAQUS® to perform the simulations.

As mentioned in the previous section, this implant is composed of a PEEK spacer and a fixation system (plate and screws) made of titanium. Table 3 sums up the material properties assigned to each part of the assembly.

Several partitions were created in the assembly in order to obtain a more homogeneous mesh. In addition, several surfaces, reference points and coordinate systems were created for the definition of interactions and forces.

Two steps were used in the simulations: one for a pre-load and a second one for the compressive preload and a moment. For each step, several 'History Output Requets' were created so that the results could be easily analyzed.

A reference point placed in the center of the upper surface of the L4 vertebra was coupled to the entire upper surface of the same vertebra so that all the loads applied in this point could be homogeneously distributed to the entire surface. For the short-term simulations, the bone-screws interactions were modelled as being fully bonded with a 'Tie' constraint, while the spacer-bone interactions were characterized as surface-to-surface contacts with a friction coefficient of 0.8. On the one hand, the constraint used for the bone-screws interaction ensures that the two surfaces being tied do not have any relative motion between them, mimicking an intimate bone-screw purchase. On the other hand, with the high friction coefficient used for the spacer-bone interactions, the behavior of a serrated surface can be simulated while avoiding long simulation times [21]. The same interaction as in the short-term simulations was defined for the bone-screws interactions in the long-term cases. However, the major difference

Table 2: Description of the original and the new designs.

Design	Description
Original	Original design with four screws: two on the top surface (one on the right diverging to the right and one on the left diverging to the left) and two on the bottom surface one on the right diverging to the right and one on the left diverging to the left).
1	New design with only two screws (one on the upper and one on the lower surfaces of the spacer) positioned in the center of the cage, both pointing to the center of the vertebral body.
2	New design with three screws: one on the right of the top surface diverging to the right and two on the bottom (one on the right diverging to the right and one on the center pointing to the center of the vertebral body).
3	New design with three screws: two on top (one on the right diverging to the right and one on the center pointing to the center of the vertebral body) and one on the right side of the bottom surface diverging to the right.
4	New design with three screws: two on the top surface (one on the right diverging to the right and one on the left diverging to the left) and one on the center of the bottom surface pointing to the center of the vertebral body.
5	New design with three screws: two on the top surface (one on the right and one on the left, both diverging to the right) and one on the right of the bottom surface, diverging to the right
6	New design with three screws: two on the top surface (one on the right and one on the left, both diverging to the right) and one on the center of the bottom surface, diverging to the right.
7	New design with four screws: two on the top surface (one on the center pointing to the center of the vertebral body and one on the right diverging to the right) and two on the bottom surface (one on the center pointing to the center of the vertebral body and one on the right diverging to the right).

Table 3: Material properties assigned to the different parts of the Synfix-LR system.

Material	Formulation	Parameters	Reference
PEEK	Linear Elastic	E = 3600 MPa	[19]
		$\nu = 0.38$	
Titanium alloy TiAl6Nb7	Linear Elastic	E = 105000 MPa	[20]
		$\nu = 0.34$	

between the short-term and the long-term scenarios is the method used for the definition of the spacer-bone interface. For the long-term situations, the upper and lower surfaces of the spacer were tied to the lower surface of the L4 vertebra and upper surface of the L5 vertebra, respectively. This means that the cage was fully bonded to the cartilaginous endplates, simulating the bone ingrowth that starts occurring after the procedure and, consequently, the fused condition of the two adjacent vertebrae.

All the models were subjected to the same loading and boundary conditions. A combination of a 500 N compressive pre-load and several 7.5 Nm moments was used to mimic the basic physiological motions (extension/flexion, lateral bending and axial rotation) [22]. Both the compressive pre-load and the moments were applied in the reference point mentioned above. The compressive pre-load was created to simulate the action of the muscles that were not included in the FE model and the option 'Follow nodal rotation' was used to simulate this compressive pre-load as a follower load. This means that the force being applied in the upper surface of the L4 vertebra is always perpendicular to the surface. For all the simulations, the lower surface of the L5 vertebra was completely fixed by an 'Encastre' condition.

As mentioned before, the analyses were carried out with ten nodes quadratic tetrahedral elements (C3D10) and a 2.5 mm seed size.

4. Results and Discussion

As explained before, eight designs (seven new designs and the original) were tested to describe the different effects that each one produces in the instrumented segment and in the biomechanical performance of the lower lumbar spine. The parameters used for the comparison were the RoM and the contact area at the spacer-bone interfaces.

4.1. Range of motion - Short-term

As can be observed from Table 4, the predictions for the RoM of the new designs were always higher than the ones obtained for the original design. When comparing the overall performance of the several cage designs, design 7 was the one that on average (over the six moments) showed the most similar outcomes comparing with the original design. On average, the values predicted for the RoM of this design were 32% higher than the ones for the original design. It is worth mentioning that, for this design, the motions that do not require any lateral movement, extension and flexion, actually resulted in outcomes similar to those of the original design. Under extension, the predicted RoM was the same for the two designs and when a flexion moment was applied, the difference was only 0.02°(1.13%). On the contrary, the worst overall results were predicted for design 1. On average, the RoM predictions for this model were 148.49% higher than the predictions for the original design. Also for this design, the lowest difference was predicted for an extension moment (0.05°corresponding to a 13.51% difference) while the highest was predicted under a moment inducing left axial rotation (1.58°corresponding to a 316% difference).

4.2. Range of motion - Long-term

As previously mentioned, the long-term simulations intend to mimic the behavior of the L4-L5 segment after the bone ingrowth and fusion of the adjacent vertebrae.

Table 5 summarizes the numerical calculations for each design and for each physiological motion.

As can be observed from Table 5, the predictions obtained for the long-term simulations are much more favorable than the ones obtained for the short-term situation. This improvement might be related with the fact that, for the long-term simulations, all the parts are fully bonded. This constraint significantly reduces the RoM for all the models, even for those with a reduced number of screws (in relation to the original design). Despite the fact that only one new design had the same RoM prediction as the original design (design 7 under extension), the outcomes for the new designs did not show any significant increase of the RoM comparing with the original design. When comparing the overall performance of the several cage designs, the design 7 was, again, the one that on average (over the six moments) showed the most similar outcomes comparing with the original design. On average, the values predicted for the RoM of this design were only 4.90% higher than those of the original design. The extension and right axial rotation simulations were the ones for which the most favorable outcomes were predicted. Under these moments, the predicted RoM was the same as with the original design. On the contrary, the worst overall results were predicted for the design 1. On average, the RoM predictions for this model were 14.26% higher than the predictions for the original design. Also for this design, the lowest difference was predicted for an extension moment (0.02°corresponding to a 6.06% difference) while the highest was predicted under a moment inducing right lateral bending (0.07°corresponding to a 24.14% difference).

4.3. Range of motion - Discussion

In Table 6, the RoM values predicted for the intact model are summarized. In these simulations, the intact model was subjected to the same loading and boundary conditions as the instrumented models.

As expected, both the short-term and the long-term simulations resulted in lower RoM values than the intact model. This decrease of the RoM is caused by the presence of the cage and its fixation system. Moreover, a significant decrease of the RoM was also predicted for the long-term in relation to the short-term scenario. Once again, this decrease was expected and it helps understanding the long-term effects of these implants.

Regarding the best overall performance, design 7 was the one showing the most favorable results for both scenarios. These results are mostly due to the fact that this fixation system is still com-

Table 4: RoM values (in degrees) of the 8 designs for the short-term scenario and the different loading conditions: Extension (Ext), Flexion (Flx), Left/Right Axial Rotation (AR) and Left/Right Lateral Bending (LB).

	Design							
	Original (in °)	**1 (in °)**	**2 (in °)**	**3 (in °)**	**4 (in °)**	**5 (in °)**	**6 (in °)**	**7 (in °)**
Ext	0.37°	0.42°	0.40°	0.39°	0.39°	0.39°	0.39°	0.37°
Flx	1.77°	2.72°	2.33°	2.50°	2.33°	2.53°	2.44°	1.79°
Right LB	0.37°	0.73°	0.73°	0.72°	0.56°	0.65°	0.59°	0.57°
Left LB	0.41°	0.83°	0.54°	0.55°	0.62°	0.52°	0.62°	0.52°
Right AR	0.50°	2.04°	1.41°	1.65°	1.34°	1.52°	1.21°	0.87°
Left AR	0.50°	2.08°	0.90°	0.72°	1.34°	0.62°	1.36°	0.68°

posed of four screws. A different behavior can be observed between left and right movements thanks to the orientation of the screws. The fact that two screws diverge to the right while the other two are positioned in the center of the spacer, results in different effects depending if it is a left or a right motions. Despite this difference, this configuration allows the surgeon to have a less complex surgical access. Regarding the short-term situation, the biggest increase (0.37°) was predicted under right axial rotation. However, in general, the predictions for the original design and design 7 were similar. As mentioned before, its behavior for the long-term scenario was even more favorable since no significant increase was predicted in relation to the original design.

On the other hand, the bad performance of design 1 was also expected and it can be justified by the low number of screws of its fixation system. The bad performances for the short and long-term simulations make design 1 the least feasible as an alternative to the original model.

4.4. Contact area - Lower interface

This subsection presents the numerical outcomes obtained for the contact area in the lower spacer-bone interface from the FE simulations ran in ABAQUS®.

As can be observed from Table 7, most of the outcomes of the new designs are lower than the ones of the new design. However, an increase in the contact area may be observed in some specific cases, most likely due to the asymmetrical geometry of some of the new designs.

This means that, unlike what was predicted for the RoM, a new design can have both lower and higher contact areas than the original design, depending on the movement. For example, using the design 4, it was predicted that in two movements, both left and right axial rotation, the resultant contact areas were higher than the ones of the original design. However, for the other four movements, the predicted contact area was higher for the original design.

In relation to the overall performance of the seven new designs, design 7 demonstrated once again to be the one that on average (for the six movements) obtains the most similar predictions to the ones of the original design. Over the different loading conditions, the contact areas predicted for this design were, on average, 17.15% lower than the predictions of the original model. Using this design resulted in a higher contact area than the original design for two of the six movements: a 3.95% increase for extension (5.59 mm^2) and a 10.43% increase under right axial rotation (12.22 mm^2).

On the other hand, the worst overall performance was predicted for design 5. On average, the predicted contact areas for this model were 30.57% lower than the ones of the original design. The only increase in the contact area predictions was observed under a right axial rotation moment. For this movement, this design results in a 5.64% increase (6.60 mm^2) over the original design.

4.5. Contact area - Upper interface

When considering the upper spacer-bone interface, the predicted contact areas of the new designs are significantly more similar to the ones of the original design than on the lower interface. Table 8 sums up the predicted contact areas for the 8 designs and the 6 different motions.

With respect to the overall performance of the new designs, design 4 was the one that on average

Table 5: RoM values (in degrees) of the 8 designs for the long-term scenario and the different loading conditions: Extension (Ext), Flexion (Flx), Left/Right axial rotation (AR) and Left lateral bending (LB).

	Design							
	Original (in °)	**1 (in °)**	**2 (in °)**	**3 (in °)**	**4 (in °)**	**5 (in °)**	**6 (in °)**	**7 (in °)**
Ext	0.33	0.35	0.34	0.34	0.34	0.34	0.34	0.33
Flx	0.48	0.56	0.53	0.53	0.53	0.53	0.53	0.49
Right LB	0.29	0.36	0.30	0.30	0.33	0.30	0.33	0.30
Left LB	0.30	0.37	0.37	0.37	0.34	0.36	0.35	0.36
Right AR	0.26	0.28	0.27	0.26	0.27	0.26	0.28	0.26
Left AR	0.26	0.28	0.27	0.28	0.27	0.28	0.27	0.27

Table 6: RoM values (in degrees) predicted for the intact model.

Motion					
Extension (in °)	**Flexion (in °)**	**Right LB (in °)**	**Left LB (in °)**	**Right AR (in °)**	**Left AR (in °)**
11.98°	7.74°	6.77°	6.50°	6.89°	7.21°

(over the six movements) obtained the most favorable predictions. Over the different loading conditions, the contact areas predicted for this design were, on average, 5.31% higher than the predictions of the original one. In fact, the contact areas predicted for this design were higher than the ones of the original design in 5 of the 6 motions. Only under flexion is that the predicted contact area was 2.04 mm^2 for both designs. Still for design 4, the biggest increase in the contact area was predicted under a left lateral bending: 6.39 mm^2 representing an increase of 9.84%.

On the other hand, the worst overall performance was predicted for design 2. On average, the predicted contact areas for this model were 21.34% lower than the ones of the original design. Not a single increase in the contact area was predicted for the 6 motions using this design, and its worst performance was predicted to occur under right lateral bending: decrease of 50.25 mm^2.

4.6. Contact area - Discussion

Regarding the lower interface, design 7 obtained once again the most favorable results. This can again be justified by the number of screws of its fixation system. On the other hand, the bad performance of design 5 can also be due to the fact that this fixation system only includes one screw in this interface. This lack of stability leads to a bigger movement of the cage when loaded, resulting in smaller contact areas than the rest of the new designs.

In relation to the upper interface, the best results were expected for a design that includes 2 screws in this interface. The predictions of the FE simulations verified these expectations and design 4 was the one showing the most favorable results. The fact that the screws of the upper interface are placed in the same configuration as in the original design might be the cause of these results. The opposite was also expected, meaning that a design with only 1 screw on this interface was expected to be associated with the worst performance. This was again corroborated by the FE simulations that predicted the least favorable results to design 2.

One fact worth of discussion are the low contact areas predicted for all the cage designs (including the original) when comparing with the total cross-sectional area of the upper and lower surfaces of the spacer (385.25 mm^2). This decrease might be caused by the simplifications that were made to all the models, namely the non inclusion of the spikes on the upper and lower surfaces of the spacer. As mentioned before, a high friction coefficient was used on these interactions to mimic the effect of the spikes. However, this friction coefficient only affects the tangential movement of the cage, while the penetration of the spikes on the bony endplate is not considered.

Table 7: Contact area (in mm^2) of the lower spacer-bone interface of the 8 designs under different loading conditions: Extension (Ext), Flexion (Flx), Left/Right axial rotation (AR) and Left lateral bending (LB).

	Design							
	Original (mm^2)	**1 (mm^2)**	**2 (mm^2)**	**3 (mm^2)**	**4 (mm^2)**	**5 (mm^2)**	**6 (mm^2)**	**7 (mm^2)**
Ext	141.57	113.37	149.51	113.83	118.35	110.20	114.65	147.16
Flx	1.81	1.54	1.72	1.30	1.54	1.30	1.54	1.72
Right LB	78.84	43.45	45.17	24.17	42.61	24.17	38.29	47.80
Left LB	57.03	24.73	41.87	41.27	24.52	41.62	27.22	42.29
Right AR	117.11	115.30	133.11	126.09	119.49	123.71	127.66	129.33
Left AR	118.31	123.13	59.51	64.52	123.64	68.21	67.25	62.56

Table 8: Contact area (in mm^2) of the upper spacer-bone interface of the 8 designs under different loading conditions: Extension (Ext), Flexion (Flx), Left/Right axial rotation (AR) and Left lateral bending (LB).

	Design							
	Original (mm^2)	**1 (mm^2)**	**2 (mm^2)**	**3 (mm^2)**	**4 (mm^2)**	**5 (mm^2)**	**6 (mm^2)**	**7 (mm^2)**
Ext	115.17	93.47	94.90	120.85	123.96	128.43	127.55	118.35
Flx	2.04	1.60	1.35	1.78	2.04	2.04	2.04	1.78
Right LB	75.66	57.07	25.41	63.27	79.92	80.35	80.58	66.30
Left LB	64.94	37.10	62.74	65.71	71.33	64.98	65.12	63.85
Right AR	123.43	132.24	119.48	124.52	131.02	131.35	132.30	128.81
Left AR	127.76	122.51	123.18	124.11	131.10	125.75	125.41	122.81

4.7. Discussion Summary

In this study and to achieve one of the proposed goals, several parameters were studied when applying different loading conditions to an instrumented L4-L5 segment implanted with different Synfix-LR fixation systems. These different parameters were considered to be some of the most important when analyzing the biomechanical effects of the different models [22]. When proposing an alternative to the original design, the different weights of these parameters must be taken into consideration. This means that some effects are more important to the final outcome of the surgery than others. Knowing that the main goal of this type of intervention is to stabilize the instrumented segment by maintaining disc height and restricting its movement [19], one can admit that the RoM is the most important parameter to study. Considering this, design 7 (Figure 4) stands as the most viable alternative to the original design of the Synfix-LR fixation system. This design was the one obtaining the most similar results to the original model and the biggest increase predicted for this model was approximately 74% (0.37°) under right axial rotation for the short-term scenario. As mentioned above, for the long-term situation the biggest increase was of 20% (0.06°), which in practice does not affect the performance of the cage.

In general, for the contact area, a decrease was predicted in relation to the original design. This can be justified by the simplification that was done regarding the spikes on the lower and upper surfaces of the spacer. If the spikes were included, one would expect a significant increase of the predicted contact areas in relation to the values shown in this study. However, this design still showed a good overall performance, indicating that it could be a viable option to be used instead of the original configuration.

To sum up, design 7 showed that it can be used over the original design in case it significantly decreases the risk associated with the procedure. This is an option that can be worth adopted in cases in which the surgeon has a significant difficulty in correctly inserting all the four divergent screws of the original design. This performance of design 7 was already expected since its configuration is only slightly different from the original design. In addition, it was also expected that configurations with less screws (less than four) would result in a worst RoM control and lower contact areas, and a consequent lower stabilization of the instrumented segment.

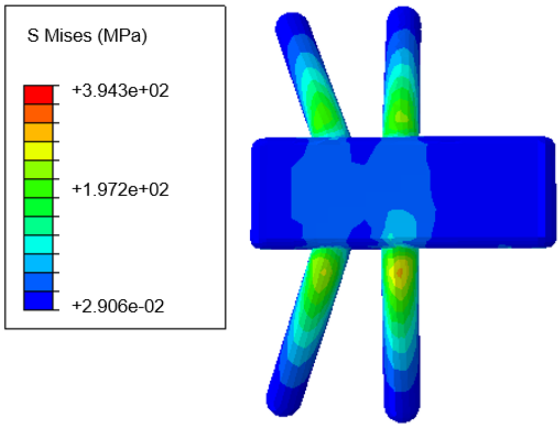

Figure 4: Stress distribution on the design 7 under flexion (anterior view).

5. Conclusions

This study raised attention to the importance of the development of new fixation systems for lumbar interbody fusion cages that require less complex surgical access. The FE simulations showed that new designs can be considered without resulting in a lower biomechanical performance, which was proved to be essential for the overall performance of both spinal adjacent levels and implant. Further developments can bring light to the wide comparison of different fixation systems in multiple time points after the surgery and its influence on the adjacent spinal levels.

5.1. Future Work

The present work presents some limitations, which could be overcome with the following scenarios for future work. Firstly, the FE model could include the entire lumbar segment of the vertebral column as well as the other anatomical structures that were not considered in this study (neural arch, ligaments, and muscles). These structures would be helpful to more correctly simulate the different motions. Secondly, and by including the entire lumbar segment, one could study the impact of a multi-level fusion on the adjacent segments. This type of intervention is usually performed in patients with a high disc degeneration at multiple levels, requiring extra stabilization of the lumbar spine. In addition, a more accurate modelling of the IVD could be done by including the collagen fibers that are naturally embedded in this structure. This would allow the model to more accurately mimic what is the natural behavior of this structure. Regarding the cage models, more designs could be developed and tested without any simplifications.

In conclusion, these additional tasks would intend to increase the accuracy of the present study.

References

[1] A. Skelton, "Low Back and Leg Pain is Lumbar Radiculopathy," 2018.

[2] A. Qaseem, T. J. Wilt, R. M. McLean, M. A.

Forciea, and Clinical Guidelines Committee of the American College of Physicians, "Noninvasive Treatments for Acute, Subacute, and Chronic Low Back Pain: A Clinical Practice Guideline From the American College of Physicians.," *Annals of internal medicine*, vol. 166, pp. 514–530, 4 2017.

[3] D. Hoy, L. March, P. Brooks, F. Blyth, A. Woolf, C. Bain, G. Williams, E. Smith, T. Vos, J. Barendregt, C. Murray, R. Burstein, and R. Buchbinder, "The global burden of low back pain: estimates from the Global Burden of Disease 2010 study," *Annals of the Rheumatic Diseases*, vol. 73, pp. 968–974, 6 2014.

[4] H. W. Khan, "Lumbar Degenerative Disc Disease," 2018.

[5] J. Peloza, "Surgery for Lower Back Pain," 2017.

[6] H. Ishihara, M. Kanamori, Y. Kawaguchi, H. Nakamura, and T. Kimura, "Adjacent segment disease after anterior cervical interbody fusion," *The Spine Journal*, vol. 4, pp. 624–628, 11 2004.

[7] A. Abbushi, M. Čabraja, U.-W. Thomale, C. Woiciechowsky, and S. N. Kroppenstedt, "The influence of cage positioning and cage type on cage migration and fusion rates in patients with monosegmental posterior lumbar interbody fusion and posterior fixation," *European Spine Journal*, vol. 18, pp. 1621–1628, 11 2009.

[8] F. H. Shen, D. Samartzis, A. J. Khanna, and D. G. Anderson, "Minimally Invasive Techniques for Lumbar Interbody Fusions," *Orthopedic Clinics of North America*, vol. 38, pp. 373–386, 7 2007.

[9] I. Teng, J. Han, K. Phan, and R. Mobbs, "A meta-analysis comparing ALIF, PLIF, TLIF and LLIF," *Journal of Clinical Neuroscience*, vol. 44, pp. 11–17, 10 2017.

[10] E. Chong, M. H. Pelletier, R. J. Mobbs, and W. R. Walsh, "The design evolution of interbody cages in anterior cervical discectomy and fusion: a systematic review," *BMC Musculoskeletal Disorders*, vol. 16, p. 99, 12 2015.

[11] G. W. Bagby, "Arthrodesis by the distraction-compression method using a stainless steel implant.," *Orthopedics*, vol. 11, pp. 931–934, 6 1988.

[12] K. Katchko, A. D. Schneider, and W. K. Hsu, "Lumbar Interbody Fusion Implant Materials," *Contemporary Spine Surgery*, vol. 18, pp. 1–8, 8 2017.

[13] F. Heuer, H. Schmidt, Z. Klezl, L. Claes, and H.-J. Wilke, "Stepwise reduction of functional spinal structures increase range of motion and change lordosis angle," *Journal of Biomechanics*, vol. 40, pp. 271–280, 1 2007.

[14] S. Naserkhaki, N. Arjmand, A. Shirazi-Adl, F. Farahmand, and M. El-Rich, "Effects of eight different ligament property datasets on biomechanics of a lumbar L4-L5 finite element model," *Journal of Biomechanics*, vol. 70, pp. 33–42, 3 2018.

[15] A. Castro, *Development of a biomimetic finite element model of the intervertebral disc diseases and regeneration*. PhD thesis, 2013.

[16] M. Thaler, E. Mayr, M. Liebensteiner, and C. M. Bach, "Injury of the right and left inferior epigastric artery during the implantation of a stand-alone ALIF cage through a left retroperitoneal approach: a case report," *Archives of Orthopaedic and Trauma Surgery*, vol. 130, pp. 31–35, 1 2010.

[17] R. C. Sasso, N. M. Best, P. V. Mummaneni, T. M. Reilly, and S. M. Hussain, "Analysis of Operative Complications in a Series of 471 Anterior Lumbar Interbody Fusion Procedures," *Spine*, vol. 30, pp. 670–674, 3 2005.

[18] "SynFix-LR System. Instruments and implants for stand-alone anterior lumbar interbody fusion (ALIF). Technique Guide," tech. rep.

[19] J. Cegoñino, A. Calvo-Echenique, and A. Pérez-del Palomar, "Influence of different fusion techniques in lumbar spine over the adjacent segments: A 3D finite element study," *Journal of Orthopaedic Research*, vol. 33, pp. 993–1000, 7 2015.

[20] "TITAN Grade Nb TiAl6Nb7," tech. rep.

[21] S.-H. Chen, M.-C. Chiang, J.-F. Lin, S.-C. Lin, and C.-H. Hung, "Biomechanical comparison of three stand-alone lumbar cages a three-dimensional finite element analysis," *BMC Musculoskeletal Disorders*, vol. 14, p. 281, 12 2013.

[22] F. Galbusera, H. Schmidt, and H.-J. Wilke, "Lumbar interbody fusion: a parametric investigation of a novel cage design with and without posterior instrumentation," *European Spine Journal*, vol. 21, pp. 455–462, 3 2012.